ELSEVIER

Biophysical Chemistry 111 (2004) 173–181

Biophysical Chemistry

www.elsevier.com/locate/bpc

Kinetic studies of iron deposition in horse spleen ferritin using H_2O_2 and O_2 as oxidants

Thomas J. Lowery Jr.[a], Jared Bunker[a], Bo Zhang[a], Robert Costen[b], Gerald D. Watt[a,*]

[a] *Department of Chemistry and Biochemistry, Brigham Young University, C100 BNSN, Provo, UT 84602, USA*
[b] *NASA Langley Research Center, Hampton, VA 23681, USA*

Received in revised form 18 May 2004; accepted 21 May 2004
Available online 2 July 2004

Abstract

The reaction of horse spleen ferritin (HoSF) with Fe^{2+} at pH 6.5 and 7.5 using O_2, H_2O_2 and 1:1 a mixture of both showed that the iron deposition reaction using H_2O_2 is ~ 20- to 50-fold faster than the reaction with O_2 alone. When H_2O_2 was added during the iron deposition reaction initiated with O_2 as oxidant, Fe^{2+} was preferentially oxidized by H_2O_2, consistent with the above kinetic measurements. Both the O_2 and H_2O_2 reactions were well defined from 15 to 40 °C from which activation parameters were determined. The iron deposition reaction was also studied using O_2 as oxidant in the presence and absence of catalase using both stopped-flow and pumped-flow measurements. The presence of catalase decreased the rate of iron deposition by ~ 1.5-fold, and gave slightly smaller absorbance changes than in its absence. From the rate constants for the O_2 (0.044 s^{-1}) and H_2O_2 (0.67 s^{-1}) iron-deposition reactions at pH 7.5, simulations of steady-state H_2O_2 concentrations were computed to be 0.45 μM. This low value and reported Fe^{2+}/O_2 values of 2.0–2.5 are consistent with H_2O_2 rapidly reacting by an alternate but unidentified pathway involving a system component such as the protein shell or the mineral core as previously postulated [Biochemistry 22 (1983) 876; Biochemistry 40 (2001) 10832].

Keywords: Horse spleen ferritin; Iron deposition; Kinetics; H_2O_2 oxidation; Ferroxidase center

Ferritins are a class of biomolecules widely distributed in nature with spherical, protein structures 12 nm in overall diameter and interior cavities ~ 8.0 nm in diameter that control the concentration of the essential iron nutrient by selectively oxidizing Fe^{2+} and depositing it within their hollow interiors as a $Fe(OH)_3$ ferrihydrite mineral core [1–4]. Arranging 24 identical subunits with 432 symmetry in bacterial ferritin or 24 similar subunits of two types called H and L in animal ferritin produces this hollow, near spherical architecture. Considerable research has focused on elucidating the mechanism of Fe^{2+} oxidation as catalyzed by apo ferritins [5–8] and the proposal made that the H subunit has a ferroxidase center [9,10] that catalytically oxidizes Fe^{2+} to Fe^{3+}, which then migrates into the ferritin interior where hydrolysis and mineral core formation occur. The role of the L subunit in animal ferritins is less clear but some studies suggest [5] its amino acid side chains act as $Fe(OH)_3$ nucleation sites on the internal walls of the hollow ferritin interior.

The reaction between Fe^{2+} and apo ferritin in the presence of O_2 rapidly and specifically forms reconstituted holo ferritin and has been useful for investigating ferritin function in vitro. An important question that arises from such studies is what product forms from O_2 reduction? This question has received extensive study and a reported Fe^{2+}/O_2 stoichiometry of 4.0 [11] for bacterial ferritins indicates O_2 reduction to H_2O. The variable stoichiometry of <2.0–4.0 for the more extensively studied animal ferritins is proposed to arise from two distinct types of reactivity: (1) two-electron ferroxidase activity within the H subunit at low iron loadings (10–150 Fe^{2+}/ferritin) where O_2 is reduced to H_2O_2 and (2) four-electron mineral surface catalysis, where O_2 is reduced to H_2O under conditions of high iron loading [6–8,12]. Extensive stoichiometric measurements and the detection and characterization of a short-lived μ-oxo-diferric peroxo intermediate support [13–16] the view that the ferroxidase center is the site of H_2O_2 formation. While this

Abbreviations: HoSF, horse spleen ferritin; bipy, 2,2′ -bipyridine.

* Corresponding author. Tel.: +1-801-378-4561; fax: +1-801-378-5474.
E-mail address: gdwatt@chem.byu.edu (G.D. Watt).

0301-4622/$ - see front matter © 2004 Elsevier B.V. All rights reserved.
doi:10.1016/j.bpc.2004.05.008

protein-based Fe^{2+} oxidation mechanism (ferroxidase center) and the mineral core surface reaction have provided a unifying view of iron deposition in animal ferritins, recent studies have reported some deviations from this predicted reactivity [17–19].

The inability to detect free H_2O_2 in solution at low iron loading [17] prompted a reinvestigation [19] of the ferroxidase reaction and a subsequent clarification of ferritin reactivity. Measured Fe^{2+}/O_2 stoichiometries near 2.0 for horse spleen ferritin (HoSF) and rHF strongly supported the formation of H_2O_2, but direct measurements demonstrated less than predicted amounts for HoSF (10%) and rHF (30–50%). To explain these results, an earlier proposal [20] was invoked, suggesting that H_2O_2 reacts after formation with the protein shell or the mineral core [19]. That H_2O_2 quantitatively forms within 25–70 ms in frog M ferritin was confirmed by rapid freeze-quench measurements [21] and leaves little doubt of its initial formation during iron deposition. This study also established that H_2O_2 is rapidly consumed by a secondary reaction and its concentration approaches zero when all Fe^{2+} has reacted. These results add a complication to the proposed functioning of the ferroxidase center because H_2O_2 does not accumulate [17] or accumulates to low levels [19] in solution but reacts by an undefined pathway to form an unidentified protein or mineral core product [19,20]. Such behavior requires further examination to better define the reactivity of O_2 and H_2O_2 occurring at the ferroxidase center and to gain insights into the secondary reaction proposed to react with the newly formed H_2O_2.

The mechanism attributed to mineral surface catalysis was recently investigated at iron loadings of 10–400 Fe^{2+}/HoSF and the results suggested that the ferroxidase center was sufficient to catalyze this amount of iron oxidation without invoking mineral core catalysis [18]. However, a related study [22], in addition to previous reports [7,22], reaffirmed that catalysis occurs on the mineral core surface of recombinant human liver heavy and light homopolymer when large aliquots (100–800 Fe/ferritin) of iron are added. At these higher loadings, ferroxidase, mineral surface catalysis and, importantly, Fe^{2+} oxidation by H_2O_2 formed from O_2 reduction all seem to be functional during iron deposition into ferritins, but the ferroxidase center catalyzes larger amounts of Fe^{2+} oxidation than previously expected [18,23].

The results and hypotheses summarized above pose some important questions about the iron deposition reaction and suggest that further studies of both ferroxidase and mineral core reactions be extended. The proposed secondary reaction of H_2O_2 [19,20] is important to elucidate to gain a better understanding of the reactivity of the ferroxidase center itself. The reaction of H_2O_2 in the secondary reaction must be sufficiently rapid so that little reaction of H_2O_2 with Fe^{2+} occurs to consistently produce Fe^{2+}/O_2 values of 2.0–2.5 and not 4.0. We report here ongoing stopped-flow kinetic studies of iron deposition with O_2 at low iron loadings of 10–30 Fe^{2+}/HoSF, where exclusive ferroxidase reactivity is occurring, and compare the results with the reaction of iron deposition using H_2O_2. HoSF was utilized for initial studies because it is a native H–L heteropolymer that gives Fe^{2+}/O_2 values near 2.0, consistent with H_2O_2 reacting quantitatively in a secondary reaction. The results show that H_2O_2 reacts ~20-fold faster than O_2 and this reactivity has important kinetic and stoichiometric implications regarding the production and subsequent reactivity of H_2O_2 toward the protein and its mineral core.

1. Materials and methods

Apo and holo horse spleen ferritin (HoSF) were obtained from Sigma. Apo HoSF was also prepared from holo HoSF by the thioglycolic acid procedure [24] and its characteristics and stability described [17,18]. Protein concentrations were determined by the Lowry method and confirmed by the absorbance at 280 nm ($\varepsilon = 472{,}000\ M^{-1}\ cm^{-1}$) for the 24-mer [19]. The H subunit composition was estimated at 2–4 H by PAGE gel electrophoresis and 3.7 by the microcoulometric method [25,26]. Iron content of the apo and reconstituted HoSF ferritins was determined by reaction with dithionite in the presence of 2,2′-bipyridine (bipy) at 520 nm ($\varepsilon = 8400\ M^{-1}\ cm^{-1}$) or ophen at 511 nm ($\varepsilon = 9640\ M^{-1}\ cm^{-1}$). Stock solutions of 0.01 M H_2O_2 were prepared by diluting a concentrated 30% solution with cold Milli Q water and storing 1.0 ml portions at −25 °C until needed. The 1.0 ml aliquots were thawed, diluted and standardized by microcoulometry just before use. Bovine catalase was obtained from Sigma at 30 mg/ml with 47,000 units/mg. H_2O_2 was determined in iron deposition reactions by the Amplex Red method using a kit supplied by Molecular Probes, Eugene, OR [17]. Microcoulometry was used to determine H_2O_2 concentration as well as determine the total reducibility of reconstituted HoSF. A Clark O_2 electrode was used to measure O_2 concentrations and determine the Fe^{2+}/O_2 ratio during iron deposition into HoSF.

Previous studies reported [19] that thioglycolate was present (identified by its odor) in commercial apo HoSF, which could not be removed by extensive dialysis. Both Sigma apo and apo prepared from Sigma holo by the thioglycolic acid were dialyzed against or passed through desalting columns equilibrated with 0.10 M NaCl to remove sulfur containing buffer components. No odor of thioglycolate was present. These samples were analyzed for total sulfur content by inductively coupled plasma spectrophotometry and the results were identical to the sulfur content of the horse light subunit [27], indicating the absence of extraneous sulfur compounds. To determine if newly formed H_2O_2 reacts with the protein component, amino acid analysis was conducted on HoSF before and after 24 consecutive additions of 10 Fe^{2+}/addition (10 min between additions).

Table 1
Rate constants for the reaction of HoSF with O_2 and H_2O_2 in 0.025 M Mops, 0.05 M NaCl at the indicated pH values measured by stopped-flow spectrophotometry

pH 7.5	k_1 (s^{-1})	k_2 (s^{-1})
O_2	0.044 ± 0.002[a]	0.0075 ± 0.0005
H_2O_2	0.67 ± 0.03	0.074 ± 0.004
pH 6.5		
O_2	0.017 ± 0.001	0.0022 ± 0.0004
H_2O_2	0.34 ± 0.02	NA[b]

[a] The uncertainty was estimated from duplicate or triplicate measurements under the same conditions.
[b] This reaction fits well to a single exponential.

1.1. Kinetic measurements

Iron deposition was conducted at pH 6.5 and 7.5 using 0.05 M Mops, 0.05 M NaCl at ~ 5.0 μM HoSF (Fe/HoSF 10–30) under constant air saturation in the pumped flow cell previously described [18]. Stopped-flow measurements of iron deposition with O_2 in air were conducted at 1.0–5.0 μM HoSF at a Fe^{2+}/HoSF ratio of 8–30—using an Applied Photophysics Sequential SX-18MV Stopped-Flow Reaction Analyzer. The stopped-flow was contained in a nitrogen-filled Vacuum Atmospheres glove box with O_2 levels below 0.1 ppm (Nyad O_2-Monitor). A Neslab RTE-111 Refrigerated Bath/Circulator controlled the temperature (± 0.05 C) of the stopped-flow syringes and optical cell at temperatures between 10–40 °C. Kinetic measurements of $Fe(OH)_3$ core formation at 375 and 305 nm were conducted by mixing anaerobic HoSF solutions at a selected Fe^{2+}/HoSF ratio with buffer solutions containing 210 μM O_2 as measured by microcoulometry [18]. Identical stopped-flow measurements were also made under the same conditions using H_2O_2 in place of O_2.

Differential equations derived from Schemes 1 and 2 (see Discussion) and measured rate constants in Table 1 were integrated forward in time using a fixed interval fourth-order Runge Kutta scheme with Math Cad. The simulated product concentrations as a function of time were then transferred to Micro Soft Excel and the results plotted for visualization.

2. Results

2.1. HoSF kinetic reactions

The reaction of 5.4 μM HoSF with 45.2 μM Fe^{2+} (8.4 Fe^{2+}/HoSF) at pH 7.5 with 105 μM O_2 (concentration after mixing)[1] is shown as the lower curve in Fig. 1. Similar reactions were observed at 15 Fe^{2+}/HoSF but are not shown. The rate of $Fe(OH)_3$ core formation with O_2 is complete in <300 s, as previously reported under identical conditions but obtained by the pumped-flow method [18].

[1] At the elevation where these experiments were conducted (1631 m) the O_2 concentration in saturating air is 210 μM, see footnote 2 in Ref. [18].

The upper two curves show the reaction with 105 μM H_2O_2, or 105 μM H_2O_2 and 105 μM O_2 as oxidants. The rate for both is nearly identical but is increased ~ 20-fold relative to the reaction with O_2. The presence of O_2 does not enhance the rate of the O_2–H_2O_2 mixture because H_2O_2 reacts preferentially. The absorbance change for the slower reaction with O_2 reaches the same absorbance as the upper curves, suggesting that the same mineral core is formed in all cases.

The reaction was conducted as a function of H_2O_2 concentration from 100 to 300 μM and the rate increased linearly from 100 to 220 μM, indicating a first-order reaction in H_2O_2. At 250 and 300 μM the rate was no longer linear indicating the onset of saturation with this substrate. From these data, a K_m for H_2O_2 of ~ 100 μM was determined, which is comparable to a value for O_2 of 140 μM previously reported [22].

The selectivity for H_2O_2 reacting with Fe^{2+} was further investigated at pH 7.5 in Fig. 2 by initially starting the reaction at 210 μM O_2 and then midway through the reaction adding 210 μM H_2O_2. Consistent with Fig. 1, the rate of Fe^{2+} deposition is increased by H_2O_2, which demonstrates a clear preference for Fe^{2+} oxidation by H_2O_2 when it is free in solution. The reaction with H_2O_2

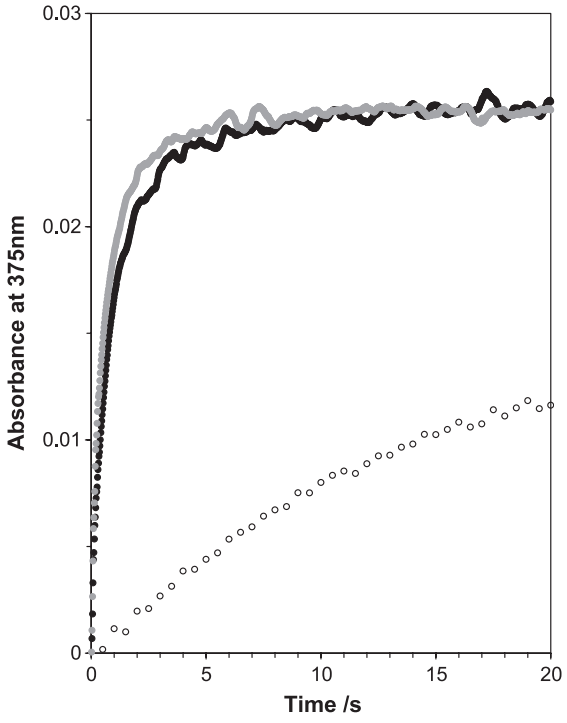

Fig. 1. The lower curve is a stopped-flow trace for the reaction of Fe^{2+} and 4.5 μM HoSF (Fe^{2+}/HoSF = 8.4) in 0.05 M Mops, 0.050 M NaCl pH 7.5 with 210 μM O_2 in the same buffer at 25.0 C. The Fe^{2+} and HoSF were present in one syringe of the stopped-flow and the other syringe contained 210 μM O_2 in buffer. The upper curve is for an identical reaction except one syringe contained 210 μM O_2 and 210 μM H_2O_2. The middle curve is for an identical reaction except one syringe contained only 210 μM H_2O_2. Identical progress curves were obtained if HoSF and O_2 were in one syringe and mixed with Fe^{2+} in anaerobic buffer contained in the other.

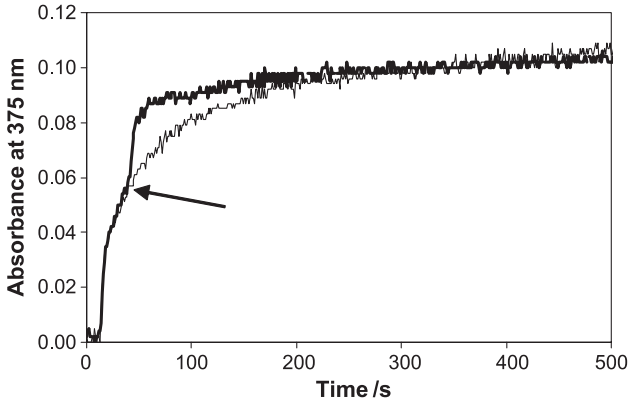

Fig. 2. The lower curve is the reaction of 8.0 μM HoSF in 0.05 M Mops, 0.050 M NaCl pH 7.5 with 80 μM Fe^{2+}. The upper curve is a duplicate of the lower curve until 210 μM H_2O_2 was added 25 s after the reaction was initiated. Similar results were obtained at pH 6.5 except the initial reaction with O_2 and H_2O_2 is ~ twofold slower.

in Fig. 1 is complete within ~ 10 s, whereas in Fig. 2 the reaction appears to be slower (~ 25 s) with a slow final drift. A slow final drift is also present in Fig. 1 but is not apparent because of the narrow time window of presentation. This slow drift is in part due to a secondary reaction occurring with both O_2 and H_2O_2 as oxidants (see below). Similar reactions were conducted at pH 6.5 (not shown) and show that the reaction rate with both H_2O_2 and O_2 decreases ~ twofold.

After iron deposition was complete with H_2O_2, HoSF was centrifuged to remove any precipitated protein or $Fe(OH)_3$ (none was found), separated by Sephadex G-25 chromatography and the iron content of HoSF was measured. In all cases, >95% of the added iron was found in the HoSF fraction, indicating that H_2O_2 specifically oxidized all added iron to form the $Fe(OH)_3$ mineral core. Both apo and reconstituted holo HoSF (30 and 100 Fe/HoSF) at 5.0 μM were reacted for 1 h with 100 μM H_2O_2 and a 15% and a 23% decrease in H_2O_2 concentration was measured, respectively, relative to a buffer control. These results are similar to previous measurements [17,23] indicating that little reaction of H_2O_2 occurs with either protein.

Attempts were made to fit the lower curve in Fig. 1 to a first-order reaction but, it was best fit to two exponentials, with k_1 (0.044 s^{-1}) about ~ six times faster than k_2 (0.0075 s^{-1}). These results are in agreement with independent measurements conducted under identical conditions using an optical flow cell [18]. Analysis of the H_2O_2 reactions, showed that two exponentials also were required with k_1 (0.67 s^{-1}) ~ nine times faster than k_2 (0.074 s^{-1}). Two reactions describe both the O_2 and the H_2O_2 oxidation reactions with each set of rate constants differing by a factor of 6–9. However, the reactions with H_2O_2 increased each rate constant ~ 20-fold depending on pH relative to the corresponding reactions with O_2. Table 1 gives the rate constants determined for HoSF iron deposition reaction.

2.2. Temperature

Fig. 3 shows a series of progress curves at different temperatures for the iron deposition reaction with O_2. A similar set of reactions was observed using H_2O_2 and as shown in the inset is ~ 20-fold faster than with O_2. Two reactions were required to fit the progress curves for each

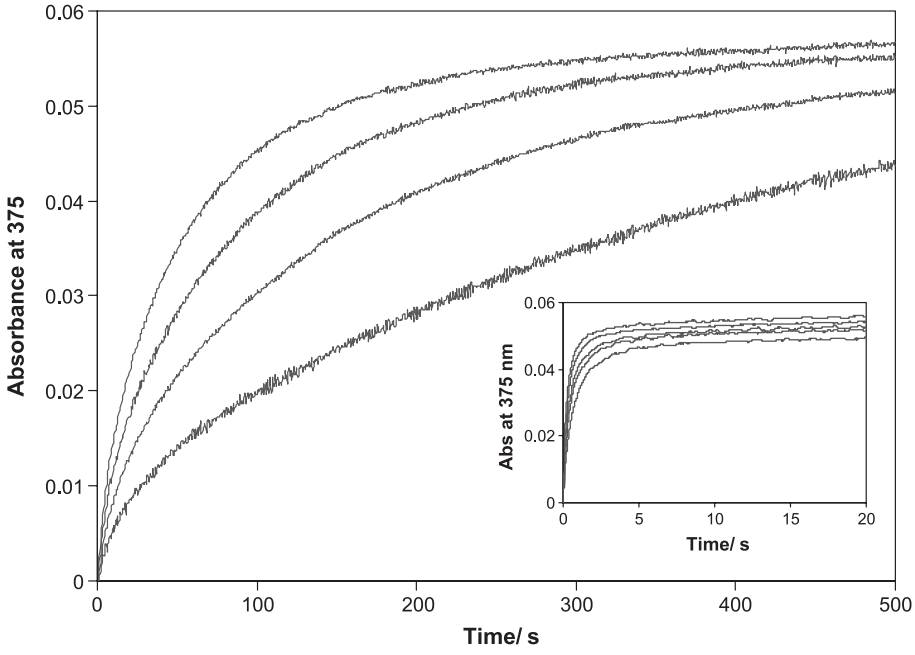

Fig. 3. The reaction of 5.4 μM HoSF with 210 μM O_2 at a Fe^{2+}/HoSF ratio of 15 in 0.050 M Mops, 0.050 M NaCl pH 7.5 at 15, 20, 25 and 35 °C (bottom to top). The inset shows the same reaction except with H_2O_2 under the same conditions.

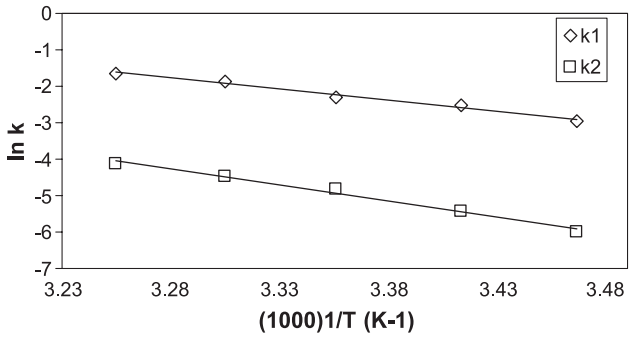

Fig. 4. The Arrhenius plot of the data in Fig. 3 for O_2. The upper line corresponds to the faster reaction (k_1) and the lower line to the slower reaction (k_2).

oxidant at each temperature. Fig. 4 shows the Arrhenius plot for the iron deposition reaction conducted with O_2 and Table 2 summarizes the activation parameters for both the O_2 and H_2O_2 reactions. Uniform activation energies were obtained over the 10–40 °C interval, indicating that the two-reaction fit for each oxidant represents the reactivity well.

2.3. pH effects

The iron deposition reaction with O_2 at pH values of 6.5, 6.75, and 7.5 are shown in Fig. 5. The rate increases with increasing pH for both O_2 and H_2O_2 and the final absorbance is similar in all cases, indicating that a common mineral core is formed. Two first-order rate constants are required to fit the progress curves at each pH but the contribution of each reaction to the total changes with pH. The reaction at pH 6.5 is slowest because the reaction with the smaller rate constant (k_2) makes a larger contribution to the total rate. The reaction is faster at pH 7.5 because the faster rate constant (k_1) is more dominant.

2.4. Catalase reaction

Catalase [5–8] changes the Fe^{2+}/O_2 stoichiometry at low iron loading from values of ~2.0 to ~4.0. The explanation is that H_2O_2 initially formed was decomposed by catalase ($H_2O_2 = 1/2\ O_2 + H_2O$) and the resulting O_2 recycles to oxidize more Fe^{2+} yielding Fe^{2+}/O_2 values of ~4.0.

Table 2
Activation parameters for the iron deposition reaction at pH 7.5 using O_2 and H_2O_2 as oxidants

	E_a (kJ/mol)	$\Delta H^{\pm}$ (kJ/mol)	$\Delta S^{\pm}$ (kJ/K mol)
O_2 reaction			
k_1	50.6 ± 2.5	48.1 ± 2.5	−104 ± 9.6
k_2	73.3 ± 4.3	70.8 ± 4.3	−51.2 ± 6.3
H_2O_2 reaction			
k_1	16.8 ± 1.8	14.3 ± 2.5	−194 ± 12.6
k_2	12.2 ± 3.5	9.7 ± 1.3	−223 ± 16.3

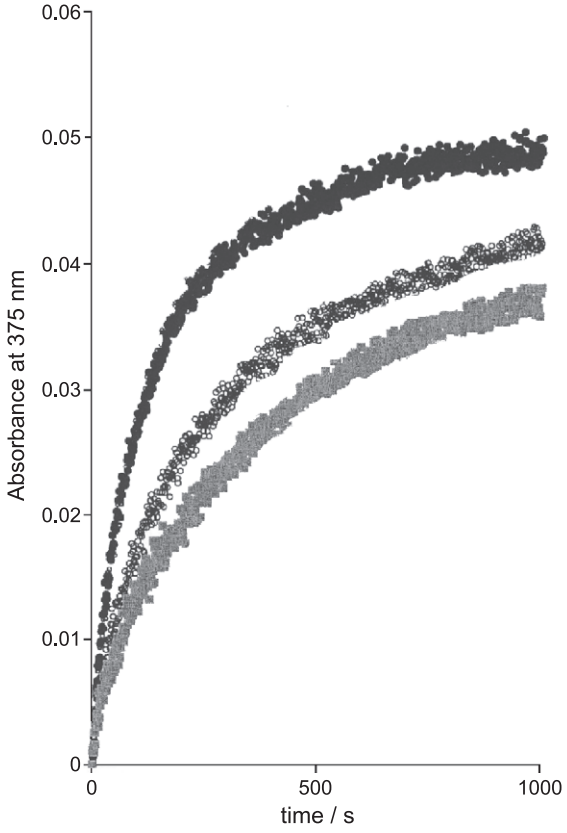

Fig. 5. The variation in rate of Fe^{2+} oxidation with pH is shown using O_2 as oxidant at pH 6.5, 6.75 and 7.5, bottom to top. The buffers were 0.05 M Mops, 0.050 M NaCl at the indicated pH values and all reactions were conducted by stopped-flow spectrophotometry. The HoSF concentration was 5.0 μM at a Fe^{2+}/HoSF ratio of 15 for all experiments.

Stopped-flow measurements at pH 7.5 for oxidation of 10 Fe^{2+}/HoSF with O_2 were conducted in the presence and absence of catalase (see inset in Fig. 6). The rate is slightly slower in the presence of catalase producing a slightly lower absorbance (~5–10). Fig. 1 (and the inset to Fig. 6) only shows the kinetic effects of a single addition of 8–15 Fe/HoSF because sequential additions to the same sample are not readily conducted. Fig. 6 compares five sequential additions of 15 Fe^{2+}/HoSF in the presence and absence of catalase using the pumped-flow method. Consistent with the stopped-flow results, catalase causes a minor decrease in the rate of iron deposition for the first reaction but decreases subsequent reactions by a factor of 1.5. The absorbance change for the first step in the presence and absence of catalase is similar but becomes smaller in the presence of catalase than in its absence for additions 2–5. Fe^{2+}/O_2 values of ~3.5 and ~2.5 were measured for all reaction steps in Fig. 6 in the presence and absence of catalase, respectively. The slowing of the reaction, a Fe^{2+}/O_2 value near 3.5 in the presence and a value of 2.5 in its absence suggest that catalase prevents a competing, but undefined, reaction from occurring. This occurs presumably by rapid destruction of H_2O_2 by catalase before the competing reaction can utilize H_2O_2 or by catalase inhibiting the

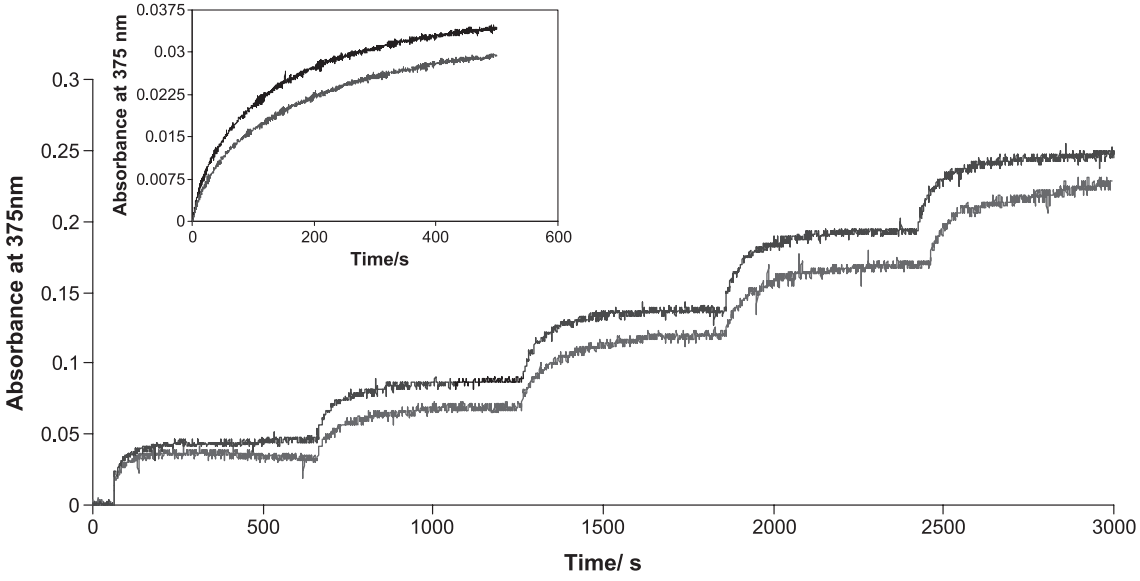

Fig. 6. The sequential addition of 10 Fe^{2+}/HoSF was conducted in the presence (lower light line) and absence of catalase (upper dark line) at pH 7.5 in the pumped-flow cell. The HoSF and Fe^{2+} concentrations were 5.0 and 50 μM, respectively in 0.05 M Mops, 0.050 M NaCl pH 7.5 and the temperature was 25 °C. The inset shows stopped-flow traces for the reaction of 81 μM Fe^{2+} and 5.4 μM HoSF with 210 μM O_2 in 0.05 M Mops, 0.050 M NaCl pH 7.5 in the presence (upper curve) and absence (lower curve) of 2.1 μM catalase.

secondary reaction in some other way. The smaller rate decrease by catalase for the first step agrees with previous results [18] showing that the first 10–30 Fe/HoSF has distinct optical, kinetic, pH and HoSF mobility properties and represents formation of a distinct species than that formed by later Fe^{2+} oxidation steps.

3. Discussion

Iron deposition with either O_2 or H_2O_2 as oxidant consists of two apparent first order reactions whose rates differs by a factor of 6–9 [18]. However, for H_2O_2, the iron deposition reaction is >20 times faster (depending on pH) than the reaction with O_2. Rapid Fe^{2+} oxidation by H_2O_2 was predicted thermodynamically and previously observed [17,29]. When the reaction is conducted at different temperatures, Fig. 4 shows that the two-reaction behavior persists, is well defined and allows the determination of the activation energy for both reactions for each oxidant (Table 2). E_a, $\Delta H^{\pm}$ and $\Delta S^{\pm}$ values of 36.3, 34.2 kJ/mol and −108 J/mol K were recently measured for iron deposition in HoSF assuming a single reaction [6] and are similar to the results in Table 1 except the reaction reported here was resolved into two separate reactions.

This two-reaction behavior is also apparent with pH variation. The rate constants remain invariant but the relative contributions they make to the overall reaction rate varies with pH (Fig. 5). At low pH the slower (k_2) reaction is most significant while at high pH the faster (k_1) reaction becomes dominant. This two-reaction behavior was previously described [18] and the suggestion made that the faster reaction is H-subunit catalyzed iron deposition and the second and slower reaction corresponded to iron oxidation catalyzed by the L-subunit [18]. The reaction with O_2 is characterized by large enthalpies of activation and negative entropies of activation, whereas, the reaction with H_2O_2 occurs with much smaller activation enthalpies and negative entropies twice the magnitude of the O_2 reaction.

With either O_2 or H_2O_2 as oxidant, all added iron is deposited into the HoSF interior but with H_2O_2 the overall rate of the iron deposition reaction is increased by a factor of ~20 at pH 7.5 compared to the O_2 reaction. This observation has important consequences in understanding the Fe^{2+}/O_2 stoichiometry of ~2.0 measured by various groups [5–8] between pH 6.5 and 7.5 and at low iron loadings of 10–150. These extensive stoichiometric results suggest that H_2O_2 is a reaction product of O_2 reduction but only trace [17] to low levels have been actually observed [19,20]. To explain the absence of H_2O_2 formation, it was proposed [19,20] that H_2O_2 initially forms but rapidly reacts with a system component (the protein shell or the mineral core) in some unspecified manner, although a number of specific reactions were previously considered and viewed unlikely [17]. This proposed reactivity of H_2O_2 is important to elucidate because if the protein shell is the locus of H_2O_2 reactivity, the cumulative effect of multiple Fe^{2+} additions at low Fe/HoSF levels could lead to extensive and irreparable damage to the protein structure and alter catalytic function. However, this was not observed in the present study for 24 consecutive additions because the amino acid analysis on this protein did not show significant variation relative to unreacted HoSF, making the protein shell an unlikely site for reaction. If the mineral core is the locus of

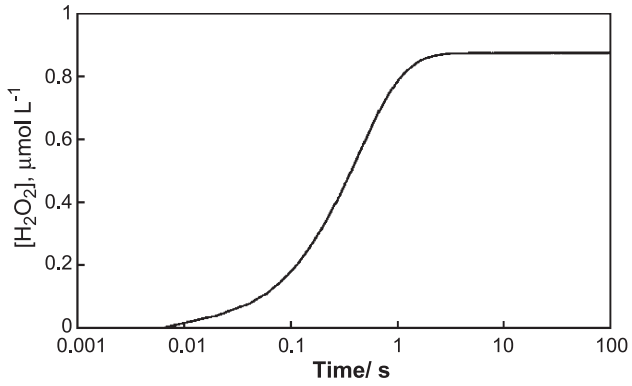

Fig. 7. Simulated H_2O_2 production as a function of time, assuming Scheme 1 and the rate constants of 0.044 and 0.67 s^{-1} for iron deposition using O_2 and H_2O_2 as oxidants, respectively. Initial conditions were the O_2 concentration held constant at 210 μM, HoSF concentration 5.0 μM, and Fe^{2+} concentration is 50 μM.

the H_2O_2 reactivity, then reconstituted mineral core might have properties different than the native core.

The present study was undertaken to compare the kinetic behavior of iron deposition using both O_2 and H_2O_2 as oxidants to better characterize the iron deposition reaction with H_2O_2. From these results, simulations were run to test possible reaction schemes that may illuminate how H_2O_2 is formed and is consumed.

Scheme 1 is a useful starting point to evaluate the fate of H_2O_2. For reactions (1) and (2), we assume that H_2O_2 is formed and immediately reacts with excess Fe^{2+} to form mineral core as shown by reaction (2).

While Scheme 1 is consistent with the kinetic results in Figs. 1 and 2, it cannot be correct because reaction (3) predicts a Fe^{2+}/O_2 stoichiometry of 4.0 and not 2.0–2.5, as measured.

Scheme 1 was, nevertheless, further evaluated as shown in Fig. 7, which is a simulation of H_2O_2 formation as a function of time using the measured rate constants at pH 7.5 obtained from Fig. 1 at 210 μM O_2. This figure shows that H_2O_2 initially begins at zero concentration when Fe^{2+} is added, builds to a maximum level near 0.90 μM and remains constant with time after all Fe^{2+} is finally oxidized at ~ 5.0 s. Fig. 7 makes three predictions that are inconsistent with experimental observation. The first is that H_2O_2 reaches a maximum concentration of 0.90 μM at 1.0 s and remains constant. The second is that Fe^{2+} is depleted [or $Fe(OH)_3$ is formed] faster than experimentally observed in Fig. 1. The third is the Fe^{2+}/O_2 stoichiometry is 4.0 and not the measured value of 2.0–2.5. That H_2O_2 is predicted to be

$$2Fe^{2+} + O_2 + 6\,H_2O \rightarrow 2\,Fe(OH)_3 + H_2O_2 + 4H^+ \quad (1)$$

$$2Fe^{2+} + H_2O_2 + 4\,H_2O \rightarrow 2\,Fe(OH)_3 + 4\,H^+ \quad (2)$$

$$4Fe^{2+} + O_2 + 10\,H_2O \rightarrow 4Fe(OH)_3 + 8\,H^+ \quad (3)$$

Scheme 1.

$$2Fe^{2+} + O_2 + 6\,H_2O \rightarrow 2\,Fe(OH)_3 + H_2O_2 + 4H^+ \quad (4)$$

$$2X + H_2O_2 \rightarrow 2XOH \quad (5)$$

$$2Fe^{2+} + O_2 + 2X + 6H_2O \rightarrow 2\,Fe(OH)_3 + 2XOH + 4H^+ \quad (6)$$

Scheme 2.

present at the end of the reaction, although Fe^{2+} reacts much faster with H_2O_2 than with O_2 is a consequence of a concentration differential. O_2 remains constant at 210 μM whereas H_2O_2 is produced only at < 1.0 μM concentrations and this low H_2O_2 concentration keeps the rate for this reaction lower than that with competing O_2 which is 20-fold slower but ~ 200 times higher in concentration. Scheme 1 does not represent the observed reactivity but the conclusions arrived at are useful because they support the proposal [19,20] of a secondary reaction, which rapidly consumes all H_2O_2 and not the results shown in Fig. 7. This secondary reaction must occur more rapidly (>10 times) than reaction (2), diverts all H_2O_2 into the secondary reaction, causes the Fe^{2+}/O_2 stoichiometry to be 2.0–2.5 and decreases H_2O_2 production below its detection level.

Scheme 2 is a modified version of Scheme 1, formed by replacing reaction (2) with reaction (5) in which X is the unidentified system component previously postulated [19,20]. Reaction (5) is used only as an illustration to discuss the kinetic and stoichiometric consequences of X reacting with newly formed H_2O_2 because the actual reactant is not known [19,20].

The predicted Fe^{2+}/O_2 and H^+/Fe^{2+} stoichiometries for reaction (6) are both 2.0 in agreement with previous measurements[2] [7]. Stoichiometries near 2.0 require that reaction (5) must be >10-fold faster than reaction (2), so that it out competes reaction (2). Reaction (2) is already ~ 20 times faster than reaction (1), so reaction (5) is a rapid reaction with a rate constant of ~ 6.7 s^{-1}.

Fig. 8 describes simulated reactivity for Fe^{2+} oxidation at constant O_2 concentration of 210 μM at pH 7.5, assuming that H_2O_2 immediately reacts with solution component X in preference to Fe^{2+}. What is apparent is that the Fe^{2+} concentration reaches zero [or $Fe(OH)_3$ reaches a maximum] at ~ 180 s (see inset), in close agreement with the results in Figs. 1 and 2. The concentration of X decreases (or XOH increases to a maximum) also within ~ 180 s and is correlated with the corresponding iron species (this result is not shown). The H_2O_2 concentration starts at zero, builds rapidly to a maximum of ~ 0.45 μM at ~ 1.0 s, and remains relatively constant for ~ 5–10 s before it declines to zero at 100 s. The maximum predicted steady-state concentration of H_2O_2 is just above the detection limit for

[2] All oxo transfer reactions leading to aldehydes, ketones, alcohols, acids, N-oxides and peroxo compounds are consistent with reaction (5). Reactions such as $X + H_2O_2 + H^+ = XOH + H_2O$ give H^+/O_2 of 3.0 and H^+/Fe^{2+} of 1.5, not the measured values of 4.0 and 2.0.

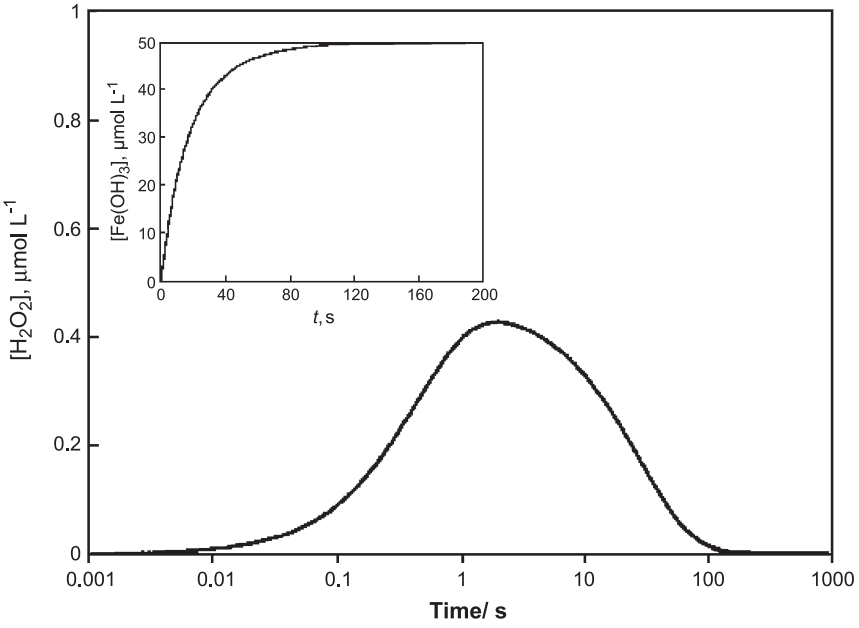

Fig. 8. Simulated H_2O_2 production assuming Scheme 2 as a function of time using the rate constants in Fig. 7 and assuming the rate constant for reaction (5) is 6.7 s^{-1}. The initial conditions were as in Fig. 7.

Amplex Red (0.18–0.25 μM) [17,19] at 1–10 s and falls to zero. This behavior explains why Lindsay et al. [17] were not able to measure H_2O_2 during the iron deposition reaction with HoSF when the reaction was sampled 10–30 s after Fe^{2+} addition.

By including Amplex Red into the iron deposition mixture, H_2O_2 was measured with HoSF at ~ 10% of the expected amount and could represent H_2O_2 formation [19] as predicted in Fig. 8. However, care must be exercised in interpreting H_2O_2 formation by this procedure because Amplex Red reacts with Fe^{2+} giving a false positive H_2O_2 response as previously reported [17].

Direct oximetric measurements [8,19] report Fe^{2+}/O_2 values near 2.0 and a slow release of O_2 after iron deposition is concluded, which was attributed to decomposition of H_2O_2 by inherent catalase activity. If catalase is added immediately following iron deposition, measurable O_2 is released from HoSF and up to 50% of the O_2 initially consumed is released in recombinant H ferritins [8,23]. These oximetry measurements are curious and appear inconsistent with the results in Fig. 8 based on the postulate that H_2O_2 is totally consumed by reaction (5). Complete reaction of H_2O_2 by reaction (5) to give a Fe^{2+}/O_2 ratio of ~ 2.0 and the release of O_2 upon addition of catalase seem mutually exclusive unless peroxo species other than H_2O_2 may be responsible for O_2 release. The presence of such a species was deemed unlikely from previous results [17].

Details of reaction (5) remain elusive even after extensive study. Fe^{2+}/O_2 stoichiometries near 2.0 have been observed using native ferritins, and recombinant H ferritins from human liver and bullfrog [5–8]. A value near 2.0 was also reported using recombinant human L ferritin [23]. The ferroxidase center in animal ferritins is the presumed site of H_2O_2 formation, which should then be consumed by reaction (5). However, stoichiometric studies using animal ferritins composed solely of H subunits containing the ferroxidase center, native ferritins composed of both H and L subunits, recombinant L ferritin devoid of the ferroxidase center and H ferritins with the ferroxidase centers removed have not clarified the identity of X associated with reaction (5). Surprisingly, values of 4.0 have been reported for *Escherichia coli* ferritin [11], a 12-subunit ferritin from *Listeria innocua* [28] and with *Azotobacter vinelandii* bacterial ferritin (unpublished observations). The nature of the reaction represented by reaction (5) becomes all the more important in understanding the HoSF iron deposition reaction and is being examined using recombinant H and L ferritins.

In other experiments, reported both here and previously [17], it was found that H_2O_2 does not react with apo or holo HoSF (containing 20–100 Fe) at a rate comparable to reaction (2) or (5). This same result was reported independently [19,20,23]. When H_2O_2 is added to either apo or holo HoSF, its concentration only slowly declines over a period of minutes or hours, apparently due to weak inherent catalase activity, and not milliseconds required by reaction (5). This result makes unlikely the view [19] that reaction (5) represents released H_2O_2 reacting with the protein shell or the mineral core. However, these experiments do not preclude the possibility that H_2O_2 is produced and reacts locally in a manner not possible by externally added H_2O_2 but the following discussion makes this possibility seem unlikely.

For 24 additions of 10 Fe^{2+}/HoSF reported previously [17] and here, where the ferroxidase center is catalyzing all Fe^{2+} oxidation, all additions gave identical rates and stoichiometric values of ~2.5 Fe^{2+}/O_2, indicating that reaction (5) was the dominant H_2O_2-consuming reaction. These results demonstrate that 240 Fe^{2+} were incrementally oxidized, 120 H_2O_2 were formed and reacted according to reaction (5), yet the protein reactivity was not diminished. If 120 H_2O_2 react locally with the protein shell, considerable protein inactivation would be expected but protein activity remained constant. This suggests that the protein shell is not the site of H_2O_2 reactivity, a conclusion supported by amino acid analysis, which showed no change in the amino acid composition.

The use of catalase has been important in establishing that H_2O_2 is formed free in solution [5–8,11] by showing that the Fe^{2+}/O_2 stoichiometry changes from ~2.0 in its absence to 4.0 in its presence. When H_2O_2 is initially produced it is presumably decomposed by catalase to O_2, preventing reaction (5) from occurring, and allowing the released O_2 to recycle. This sequence of reactions predicts that the rate of Fe^{2+} oxidation will be independent of the presence or absence of catalase because reaction (5) is much faster than rate-limiting reaction (1) and reaction (5) is responsible for Fe^{2+}/O_2 stoichiometries <4.0. Fig. 6 shows this is the case except for the first addition, which is slowed by catalase. The reason is not known but is consistent with other behavior showing that the first addition of Fe^{2+} to apo HoSF is distinct from behavior for later additions [18].

Acknowledgements

This research was partly supported by the Undergraduate Research Program of the College of Mathematics and Physical Science at Brigham Young University.

References

[1] P.M. Proulx-Curry, N.D. Chasteen, Molecular aspects of iron uptake and storage in ferritin, Coord. Chem. Rev. 144 (1995) 347–368.
[2] G.C. Ford, P.M. Harrison, D.W. Rice, J.M.A. Smith, A. Treffry, J.L. White, J. Yariv, Ferritin design and formation of an iron storage molecule, Philos. Trans. R. Soc. Lond., Ser. B. 304 (1984) 551–566.
[3] P.M. Harrison, P. Arosio, The ferritins: molecular properties, iron storage function and cellular regulation, Biochim. Biophys. Acta 1275 (1996) 161–203.
[4] G.S. Waldo, E.C. Theil, in: K.S. Suslick (Ed.), Comprehensive Supra-Molecular Chemistry, vol. 5, Pergamon, Oxford, UK, 1996, pp. 65–89.
[5] B. Xu, N.D. Chasteen, Iron oxidation chemistry in ferritin. Increasing Fe/O2 stoichiometry during core formation, J. Biol. Chem. 266 (1991) 19965–19970.
[6] S. Sun, P. Arosio, S. Levi, N.D. Chasteen, Ferroxidase kinetics of human liver apoferritin recombinant H-chain apoferritin and site-directed mutants, Biochemistry 32 (1993) 15095–15102.
[7] X. Yang, Y. Chen-Barrett, P. Arosio, N.D. Chasteen, Reaction paths of iron oxidation and hydrolysis in horse spleen and recombinant human ferritins, Biochemistry 37 (1998) 9743–9750.
[8] G.S. Waldo, E.C. Theil, Formation of iron (III)-tyrosinate is the fastest reaction observed in ferritin, Biochemistry 32 (1993) 13262–13269.
[9] D.M. Lawson, A. Treffry, A.P.J. Artymiuk, P.M. Harrison, P.M.S.J. Yewdall, A. Luzzago, G. Cesareni, S. Levi, P. Arosio, Identification of the ferroxidase center in ferritin, FEBS Lett. 254 (1989) 207–210.
[10] P.D. Hempsted, A.J. Hudson, P.J. Artymiuk, S.C. Andrews, M.M.J. Banfield, J.R. Guest, P.M. Harrison, Direct observation of the iron binding sites in a ferritin, FEBS Lett. 350 (1994) 258–262.
[11] X. Yang, N.E. Le Brun, A.J. Thomson, G.R. Moore, N.D. Chasteen, The iron oxidation and hydrolysis chemistry of *Escherichia coli* bacterioferritin, Biochemistry 39 (2000) 4915–4923.
[12] I.G. Macara, T.G. Hoy, P.M. Harrison, The formation of ferritin from apoferritin kinetics and mechanism of iron uptake, Biochem. J. 126 (1972) 151–162.
[13] F. Bou-Abdallah, G.C. Papaefthymiou, D.M. Scheswohl, S.D. Stranga, P. Arosio, N.D. Chasteen, μ-1,2-Peroxobridged di-iron(III) dimer formation in human H-chain ferritin, Biochem. J. 363 (2002) 57–63.
[14] A. Pereira, W. Small, C. Krebs, P. Tavares, D. Edmondson, E. Theil, G. Huynh, Direct spectroscopic and kinetic evidence for the involvement of a peroxodiferric intermediate during the ferroxidase reaction in fast ferritin mineralization, Biochemistry 37 (1998) 9871–9876.
[15] P. Moenne-Loccoz, C. Krebs, K. Herlihy, D.E. Edmondson, E.C. Theil, G.H. Huynh, T.M. Loehr, The ferroxidase reaction of ferritin reveals a diferric μ-1,2 bridging peroxide intermediate in common with other O2-activating non-heme diiron proteins, Biochemistry 38 (1999) 5290–5295.
[16] J. Hwang, C. Krebs, G.H. Huynh, D.E. Edmondson, E.C. Theil, J.E. Penner-Hahn, A short Fe–Fe distance in peroxodiferric ferritin: control of Fe substrate versus cofactor decay? Science 287 (2000) 122–125.
[17] S. Lindsay, D. Brosnahan, G.D. Watt, Hydrogen peroxide formation during iron deposition in horse spleen ferritin using O_2 as an oxidant, Biochemistry 40 (2001) 3340–3347.
[18] S. Lindsay, D. Brosnahan, T.J. Lowery Jr., K. Crawford, G.D. Watt, Kinetic studies of iron deposition in horse spleen ferritin using O_2 as oxidant, Biochim. Biophys. Acta 1621 (2003) 57–66.
[19] G. Zhao, F. Bou-Abdallah, X. Yang, P. Arosio, N.D. Chasteen, Is hydrogen peroxide produced during iron(II) oxidation in mammalian apoferritins? Biochemistry 40 (2001) 10832–10838.
[20] D.E. Mayer, J.S. Rohrer, D.A. Schoeller, D.C. Harris, Fate of oxygen during ferritin iron incorporation, Biochemistry 22 (1983) 876–880.
[21] G.N.L. Jameson, W. Jin, C. Krebs, A.S. Perreira, P. Tavares, X. Liu, E.C. Theil, B.H. Huynh, Stoichiometric production of hydrogen peroxide and parallel formation of ferric multimers through decay of the diferic-peroxo complex, the first detectable intermediate in ferritin mineralization, Biochemistry 41 (2002) 13435–13443.
[22] S. Sun, N.D. Chasteen, Ferroxidase kinetics of horse spleen apoferritin, J. Biol. Chem. 267 (1992) 25160–25166.
[23] G. Zhao, F. Bou-Abkallah, P. Arosio, S. Levi, C. Janus-Chandler, N.D. Chasteen, Multiple pathways for mineral core formation in mammalian apoferritin. The role of hydrogen peroxide, Biochemistry 42 (2003) 3142–3150.
[24] A. Treffery, Pl.M. Harrison, The binding of iron(III) by ferritn, Biochem. J. 181 (1979) 709–716.
[25] G.D. Watt, R.B. Frankel, Redox capacity of APo mammalian ferritin, Iron Biominerals, Plenum, New York, 1992, pp. 307–313.
[26] R.K. Watt, R.B. Frankel, G.D. Watt, Redox reactions of Apo mammalian ferritin, Biochemistry 31 (1992) 9673–9679.
[27] M. Heusterspreute, R.R. Crichton, Amino acid sequence of horse spleen light ferritin, FEBS Lett. 129 (1981) 322–327.
[28] X. Yang, E. Chiancone, S. Stefanini, A. Iliari, N.D. Chasteen, Iron oxidation and hydrolysis reactions of a novel ferritin from *Listeria innocua*, Biochem. J. 349 (2000) 783–786.
[29] G. Melino, S. Stefanini, E. Chiancone, E. Antonini, A.A. Finazzi, FEBS Lett. 86 (1978) 136–138.